Supporting Information: Impact of Van der Waals interactions on structural and nonlinear optical properties of azobenzene switches

Carmelo Naim,[†,‡] Frédéric Castet,[*,‡] and Eduard Matito[*,†,¶]

†Donostia International Physics Center (DIPC), Manuel Lardizabal Ibilbidea 4, 20018 Donostia, Euskadi, Spain

‡Institut des Sciences Moléculaires (ISM, UMR CNRS 5255), University of Bordeaux, 351 Cours de la Libération, 33405 Talence, France

¶Ikerbasque Foundation for Science, 48011 Bilbao, Euskadi, Spain

E-mail: frederic.castet@u-bordeaux.fr; ematito@gmail.com

Contents

1 Performance of RI-CC2 and RI-MP2 methods for dispersion interactions

In order to verify that the choice of RI-CC2 as reference geometry is valid for the systems under investigation, we evaluated the performances of both RI-CC2 and RI-MP2 methods on the benchmark dataset Diet-GMTKN55.[S1] Among all the molecules of the set we reproduced 20 energy differences which belong to the subset of "Intramolecular noncovalent interactions", namely the molecules of Diet-GMTKN55 which also belong to the sets: ACONF, BUT14DIOL, IDISP, MCONF, PCONF21, SCONF and UPU23. The calculations have been performed using the cc-pVDZ basis set. The results are reported in Table S1. Both RI-CC2 and RI-MP2 methods reproduce the reference data to a good accuracy (the MAE is 1.93 for RI-CC2 and 1.76 for RI-MP2).

Table S1: Collection of the energies of the Intramolecular non-covalent interactions on the Diet-GMTKN55. On the first column is indicated the name of the corresponding subset, while on the second and third columns the molecules considered as reactant and product for the calculation of the energy difference. All the energies are in kcal/mol. The geometries and reference methods can be found in the reference paper.[S1]

Dataset	Reactants	Products	ΔE_{Ref}	ΔE_{RI-CC2}	ΔE_{RI-MP2}
ACONF	H_ttt	H_g+x-t+	2.63	2.78	2.79
	H_ttt	H_x+g-g-	3.08	3.26	3.29
BUt14DIOL	B1	B3	0.30	0.50	0.44
	B1	B30	2.85	4.24	4.15
	B1	B33	2.63	5.57	5.25
	B1	B39	3.06	4.71	4.58
	B1	B40	3.10	5.40	5.05
	B1	B43	3.29	4.97	4.75
	B1	B44	3.59	6.04	5.67
	B1	B54	3.15	6.04	5.67
IDISP	octane1	octane2	-1.21	4.27	3.53
MCONF	1	12	4.45	4.31	3.83
	1	21	3.11	5.60	5.38
	1	31	4.86	6.62	6.42
PCONF21	99	366	0.70	3.96	3.62
SCONF	G1	G3	6.16	-0.63	0.29
UPU23	2p	1b	2.97	1.20	1.80
	2p	1g	2.20	1.58	1.81
	2p	7a	7.26	7.43	5.80
	2p	4b	5.48	5.74	5.80
			RMSE	1.41	1.28
			MAE	1.93	1.76

2 Impact of the basis set

Table S2: *Z*-*E* energy differences (ΔE_{EZ}, kcal/mol) calculated at the RI-CC2 level using the cc-pVDZ and cc-pVTZ basis sets.

	a (R = H)	**b** (R = Me)
cc-pVDZ	11.5	10.9
cc-pVTZ	10.8	10.0
Difference	0.7	0.9

Table S3: RMSD (Å) between geometries optimized at the RI-CC2/cc-pVDZ and RI-CC2/cc-pVTZ levels for *E* and *Z* isomers.

Molecule	RMSD (*E*)	RMSD (*Z*)
a (R = H)	0.000	0.000
b (R = Me)	0.000	0.026

3 Density functional approximations

Table S4: DFT exchange-correlation functionals (DFAs) considered in this study, with the type of approximation, amount of exact HF exchange (HFX) and applied dispersion correction (Disp.).

DFA acronym	Type	% of HFX	Ref.	Disp.
PBE	pure GGA	0	S2	PBE-D3
M06L	pure GGA	0	S3	-
rPW86PBE	pure GGA	0	S4	rPW86PBE-VV
B3LYP	hybrid GGA	20	S5	B3LYP-D3
PBE0	hybrid GGA	25	S6	PBE0-D3
M06	hybrid GGA	27	S3	-
BH&H	hybrid GGA	50	S7 (G16 version)	-
M06-2X	hybrid GGA	57	S3	M06-2X-D3
M06-HF	hybrid GGA	100	S3	-
CAM-B3LYP	hybrid RS (0.33)	19 (SR), 65 (LR)	S8	CAM-B3LYP-D3
LC-ωPBE	hybrid RS (0.40)	0 (SR), 100 (LR)	S9	LC-ωPBE-D3
LC-ωPBE08	hybrid RS (0.45)	0 (SR), 100 (LR)	S4	LC-ωPBE08-VV
LC-BLYP	hybrid RS (0.47)	0 (SR), 100 (LR)	S10	-
Tα-BLYP	hybrid RS (variable)	0 (SR), 100 (LR)	S11	-
ωB97X	hybrid RS (0.30)	15.8 (SR), 100 (LR)	S12	ωB97X-D
ωB97X-D	hybrid RS (0.20)	22.2 (SR), 100 (LR)	S13	-

GGA: Generalized Gradient Approximation; RS: Range Separated (with standard range parameter ω given in Bohr^{-1}); SR: Short Range; LR: Long Range.

4 Correlation indicators for CC2 calculations

Table S5: Evaluation of D1 and I_{ND} diagnostic calculated on the optimized geometry at the CC2 level with the cc-pVDZ basis set. The D1 threshold for molecules with a potential multireference character is 0.05. In the case of I_{ND}, we can take the dissociation of the H_2 molecule as a reference. The dissociated molecule gives $I_{ND} = 0.5$, whereas $I_{ND} = 0.025$ corresponds to the equilibrium geometry of H_2 molecule.[S14] In the present case, all the molecules display $I_{ND} \leq 0.025$, and, hence, they are not expected to present large multireference character.

Isomer	*E*		*Z*	
Molecule	D1	I_{ND}	D1	I_{ND}
a (R = H)	0.046	0.023	0.053	0.024
b (R = Me)	0.049	0.022	0.053	0.022
c (R = *i*Pr)	0.049	0.021	0.051	0.021
d (R = *t*Bu)	0.050	0.021	0.052	0.021
e (R = Ph)	0.048	0.024	0.050	0.025
f (R = Cy)	0.050	0.020	0.051	0.020
g (R = Ad)	0.051	0.020	0.052	0.021

5 Geometrical parameters of *E* isomers

Table S6: Characteristic distances and angles in the *E* isomers of the investigated molecules (Figure 1), as calculated at the RI-CC2, RI-MP2 and HF methods levels.

Molecule	d_{NN}[Å]	d_{NC}[Å]	θ_{NNC}[°]	ϕ_{CNNC}[°]
HF/cc-pVDZ				
a (R = H)	1.22	1.43	116	180
b (R = Me)	1.22	1.43	116	180
c (R = *i*Pr)	1.22	1.43	116	180
d (R = *t*Bu)	1.22	1.43	116	180
e (R = Ph)	1.22	1.43	116	180
f (R = Cy)	1.22	1.43	116	180
g (R = Ad)	1.22	1.43	116	180
RI-MP2/cc-pVDZ				
a (R = H)	1.28	1.43	113	180
b (R = Me)	1.28	1.42	113	180
c (R = *i*Pr)	1.28	1.42	113	180
d (R = *t*Bu)	1.28	1.42	113	180
e (R = Ph)	1.28	1.42	113	180
f (R = Cy)	1.28	1.42	113	180
g (R = Ad)	1.28	1.42	113	180
RI-CC2/cc-pVDZ				
a (R = H)	1.28	1.43	113	180
b (R = Me)	1.29	1.43	113	180
c (R = *i*Pr)	1.29	1.43	113	180
d (R = *t*Bu)	1.29	1.42	113	180
e (R = Ph)	1.29	1.43	113	180
f (R = Cy)	1.29	1.42	114	180
g (R = Ad)	1.29	1.42	113	180

6 RMSD analysis without hydrogens

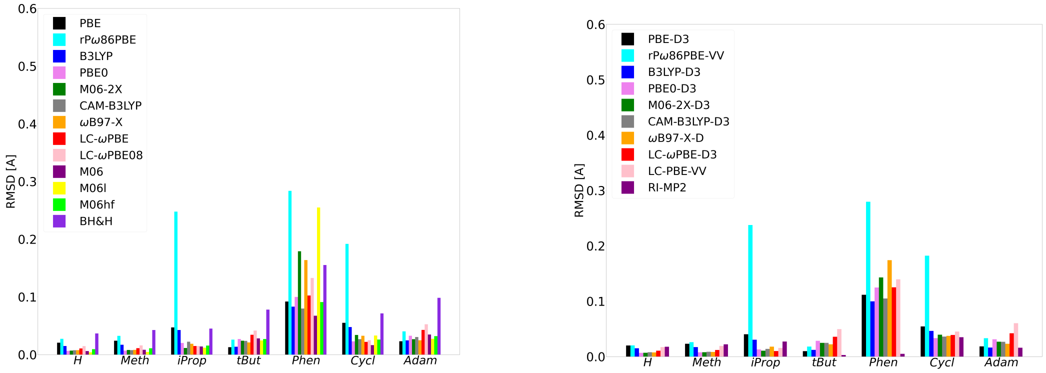

(a) (b)

Figure S1: RMSD without hydrogens between DFT and CC2 geometries for *trans* isomers, calculated using DFAs without (left) and with (right) dispersion corrections. RI-MP2 results are also shown for comparison.

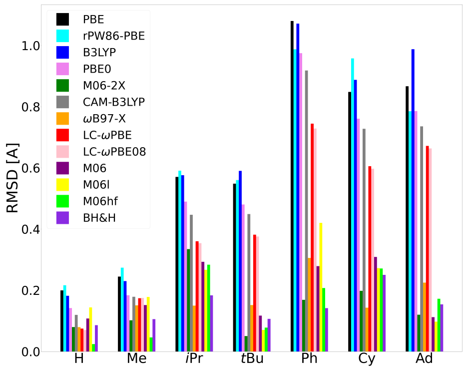

Figure S2: RMSD without hydrogens between DFAs and CC2 geometries for *cis* isomers, calculated using DFAs without dispersion corrections. RI-MP2 results are also shown for comparison.

Table S7: RMSD without hydrogens (Å) between geometries optimized using DFAs with and without dispersion corrections (in parenthesis) for *E* and *Z* isomers.

Molecule	Approx.	RMSD (*E*)	RMSD (*Z*)
a (R = **H**)	PBE(D3)	0.00	0.04
	rPW86PBE(VV)	0.00	0.00
	PBE0(D3)	0.00	0.04
	B3LYP(D3)	0.00	0.00
	M06-2X(D3)	0.00	0.00
	CAM-B3LYP(D3)	0.00	0.00
	LC-ωPBE(D3)	0.00	0.05
	LC-ωPBE(VV)	0.00	0.00
	ωB97X(D)	0.00	0.01
b (R = **Meth**)	PBE(D3)	0.00	0.07
	rPW86PBE(VV)	0.00	0.00
	PBE0(D3)	0.00	0.07
	B3LYP(D3)	0.00	0.00
	M06-2X(D3)	0.00	0.01
	CAM-B3LYP(D3)	0.00	0.00
	LC-ωPBE(D3)	0.00	0.01
	LC-ωPBE08(VV)	0.00	0.00
	ωB97-X(D)	0.00	0.05
c (R = **iProp**)	PBE(D3)	0.01	0.52
	rPW86PBE(VV)	0.00	0.00
	PBE0(D3)	0.01	0.45
	B3LYP(D3)	0.01	0.00
	M06-2X(D3)	0.00	0.04
	CAM-B3LYP(D3)	0.01	0.44
	LC-ωPBE(D3)	0.01	0.00
	LC-ωPBE08(VV)	0.00	0.00
	ωB97-X(D)	0.00	0.12

Molecule	Approx.	RMSD (E)	RMSD (Z)
d (R = **tBut**)	PBE(D3)	0.00	0.42
	rPW86PBE(VV)	0.00	0.00
	PBE0(D3)	0.00	0.63
	B3LYP(D3)	0.01	0.00
	M06-2X(D3)	0.00	0.04
	CAM-B3LYP(D3)	0.00	0.35
	LC-ωPBE(D3)	0.00	0.38
	LC-ωPBE08(VV)	0.00	0.00
	ωB97-X(D)	0.00	0.18
e (R = **Phen**)	PBE(D3)	0.03	0.87
	rPW86PBE(VV)	0.00	0.00
	PBE0(D3)	0.03	0.79
	B3LYP(D3)	0.02	0.00
	M062X(D3)	0.04	0.04
	CAM-B3LYP(D3)	0.03	0.80
	LC-ωPBE(D3)	0.03	0.65
	LC-ωPBE08(VV)	0.00	0.00
	ωB97-X(D)	0.02	0.20
f (R = **Cycl**)	PBE(D3)	0.02	0.82
	rPW86PBE(VV)	0.00	0.00
	PBE0(D3)	0.02	0.75
	B3LYP(D3)	0.03	0.00
	M06-2X(D3)	0.01	0.03
	CAM-B3LYP(D3)	0.02	0.75
	LC-ωPBE(D3)	0.02	0.63
	LC-PBE08(VV)	0.00	0.00
	ωB97-X(D)	0.01	0.13
g (R = **Adam**)	PBE(D3)	0.01	0.79
	rPW86PBE(VV)	0.00	0.00
	PBE0(D3)	0.01	0.70
	B3LYP(D3)	0.02	0.00
	M06-2X(D3)	0.00	0.06
	CAM-B3LYP(D3)	0.01	0.61
	LC-ωPBE(D3)	0.01	0.54
	LC-ωPBE08(VV)	0.00	0.00
	ωB97-X(D)	0.01	0.22

Table S8: RMSD without hydrogens (Å) between DFAs and CC2 geometries for *E* and *Z* isomers, calculated using DFAs without and with dispersion corrections. RMSD between MP2 and CC2 geometries are also reported.

Compound	Approx.	RMSD (*E*)	RMSD (*Z*)
a (R = **H**)	RI-MP2	0.02	0.01
	PBE	0.02	0.20
	PBE-D3	0.02	0.17
	rPW86PBE	0.03	0.22
	rPW86PBE-VV	0.02	0.17
	PBE0	0.01	0.14
	PBE0-D3	0.01	0.11
	B3LYP	0.01	0.18
	B3LYP-D3	0.01	0.13
	CAM-B3LYP	0.01	0.12
	CAM-B3LYP-D3	0.01	0.08
	LC-ωPBE	0.01	0.07
	LC-ωPBE-D3	0.01	0.05
	LC-ωPBE08	0.01	0.07
	LC-ωPBE08-VV	0.02	0.04
	ωB97-X	0.01	0.08
	ωB97-X-D	0.01	0.07
	BH&H	0.04	0.09
	M06	0.01	0.11
	M06L	0.00	0.14
	M06-2X	0.01	0.08
	M06-2X-D3	0.01	0.08
	M06-HF	0.01	0.02

Compound	Approx.	RMSD (E)	RMSD (Z)
b (R = **Me**)	RI-MP2	0.02	0.06
	PBE	0.02	0.24
	PBE-D3	0.02	0.17
	rPW86PBE	0.03	0.27
	rPW86PBE-VV	0.03	0.21
	PBE0	0.01	0.18
	PBE0-D3	0.01	0.11
	B3LYP	0.02	0.23
	B3LYP-D3	0.02	0.14
	CAM-B3LYP	0.01	0.18
	CAM-B3LYP-D3	0.01	0.12
	LC-ωPBE	0.01	0.17
	LC-ωPBE-D3	0.01	0.17
	LC-ωPBE08	0.02	0.17
	LC-ωPBE08-VV	0.02	0.14
	ωB97-X	0.01	0.15
	ωB97-X-D	0.01	0.11
	BH&H	0.04	0.11
	M06	0.01	0.15
	M06L	0.01	0.18
	M06-2X	0.01	0.10
	M06-2X-D3	0.01	0.10
	M06-HF	0.01	0.05
c (R = **iPr**)	RI-MP2	0.03	0.01
	PBE	0.05	0.57
	PBE-D3	0.04	0.15
	rPW86PBE	0.25	0.59
	rPW86PBE-VV	0.24	0.30
	PBE0	0.02	0.49
	PBE0-D3	0.01	0.13
	B3LYP	0.04	0.58
	B3LYP-D3	0.03	0.12
	CAM-B3LYP	0.02	0.45
	CAM-B3LYP-D3	0.01	0.13
	LC-ωPBE	0.01	0.36
	LC-ωPBE-D3	0.01	0.36
	LC-ωPBE08	0.01	0.35
	LC-ωPBE08-VV	0.02	0.09
	ωB97-X	0.02	0.15
	ωB97-X-D	0.02	0.08
	BH&H	0.05	0.18
	M06	0.01	0.29
	M06L	0.01	0.27
	M06-2X	0.01	0.33
	M06-2X-D3	0.01	0.31
	M06-HF	0.02	0.28

Compound	Approx.	RMSD (E)	RMSD (Z)
d (R = **tBu**)	RI-MP2	0.00	0.00
	PBE	0.01	0.55
	PBE-D3	0.01	0.13
	rPW86PBE	0.03	0.56
	rPW86PBE-VV	0.02	0.09
	PBE0	0.03	0.48
	PBE0-D3	0.03	0.11
	B3LYP	0.01	0.59
	B3LYP-D3	0.01	0.09
	CAM-B3LYP	0.02	0.45
	CAM-B3LYP-D3	0.02	0.12
	LC-ωPBE	0.03	0.38
	LC-ωPBE-D3	0.04	0.08
	LC-ωPBE08	0.04	0.38
	LC-ωPBE08-VV	0.05	0.07
	ωB97-X	0.02	0.15
	ωB97-X-D	0.02	0.07
	BH&H	0.08	0.11
	M06	0.03	0.12
	M06L	0.02	0.07
	M06-2X	0.02	0.05
	M06-2X-D3	0.02	0.04
	M06-HF	0.03	0.08
e (R = **Ph**)	RI-MP2	0.01	0.02
	PBE	0.09	1.08
	PBE-D3	0.11	0.22
	rPW86PBE	0.28	0.99
	rPW86PBE-VV	0.28	0.44
	PBE0	0.10	0.97
	PBE0-D3	0.12	0.20
	B3LYP	0.08	1.07
	B3LYP-D3	0.10	0.14
	CAM-B3LYP	0.08	0.92
	CAM-B3LYP-D3	0.10	0.18
	LC-ωPBE	0.10	0.74
	LC-ωPBE-D3	0.12	0.12
	LC-ωPBE08	0.13	0.73
	LC-ωPBE08-VV	0.14	0.11
	ωB97-X	0.16	0.31
	ωB97-X-D	0.17	0.12
	BH&H	0.16	0.14
	M06	0.07	0.28
	M06L	0.26	0.42
	M06-2X	0.18	0.17
	M06-2X-D3	0.14	0.13
	M06-HF	0.09	0.21

Compound	Approx.	RMSD (E)	RMSD (Z)
f (R = **Cy**)	RI-MP2	0.03	0.01
	PBE	0.05	0.85
	PBE-D3	0.05	0.14
	rPW86PBE	0.19	0.96
	rPW86PBE-VV	0.18	0.10
	PBE0	0.02	0.76
	PBE0-D3	0.03	0.11
	B3LYP	0.05	0.89
	B3LYP-D3	0.05	0.11
	CAM-B3LYP	0.03	0.73
	CAM-B3LYP-D3	0.04	0.13
	LC-ωPBE	0.02	0.61
	LC-ωPBE-D3	0.04	0.10
	LC-ωPBE08	0.02	0.60
	LC-ωPBE08-VV	0.05	0.09
	ωB97-X	0.03	0.14
	ωB97-X-D	0.04	0.17
	BH&H	0.07	0.25
	M06	0.02	0.31
	M06L	0.03	0.27
	M06-2X	0.03	0.20
	M06-2X-D3	0.04	0.19
	M06-HF	0.03	0.27
g (R = **Ad**)	RI-MP2	0.02	0.03
	PBE	0.02	0.87
	PBE-D3	0.02	0.43
	rPW86PBE	0.04	0.79
	rPW86PBE-VV	0.03	0.20
	PBE0	0.03	0.79
	PBE0-D3	0.03	0.43
	B3LYP	0.02	0.99
	B3LYP-D3	0.02	0.42
	CAM-B3LYP	0.03	0.74
	CAM-B3LYP-D3	0.03	0.43
	LC-ωPBE	0.04	0.67
	LC-ωPBE-D3	0.04	0.43
	LC-ωPBE08	0.05	0.66
	LC-ωPBE08-VV	0.06	0.45
	ωB97-X	0.02	0.23
	ωB97-X-D	0.02	0.06
	BH&H	0.10	0.15
	M06	0.03	0.11
	M06L	0.03	0.10
	M06-2X	0.03	0.12
	M06-2X-D3	0.03	0.08
	M06-HF	0.03	0.17

Table S9: Average values of the RMSD calculations (Å) without the hydrogens for each set of molecules in E and Z isomers.

Functional	Average RMSD (E)	Average RMSD (Z)
RI-MP2	0.02	0.02
PBE	0.04	0.62
PBE-D3	0.04	0.20
rPW86PBE	0.12	0.62
rPW86PBE-VV	0.11	0.22
B3LYP	0.03	0.65
B3LYP-D3	0.03	0.16
PBE0	0.03	0.55
PBE0-D3	0.03	0.17
M06-2X	0.04	0.15
M06-2X-D3	0.04	0.13
CAM-B3LYP	0.03	0.51
CAM-B3LYP-D3	0.03	0.17
ωB97X	0.04	0.17
ωB97X-D	0.04	0.10
LC-ωPBE	0.03	0.43
LC-ωPBE-D3	0.04	0.19
LC-ωPBE08	0.04	0.42
LC-ωPBE08-VV	0.05	0.14
M06	0.02	0.20
M06L	0.05	0.21
M06-HF	0.03	0.15
BH&H	0.08	0.15

7 RMSD analysis with hydrogens

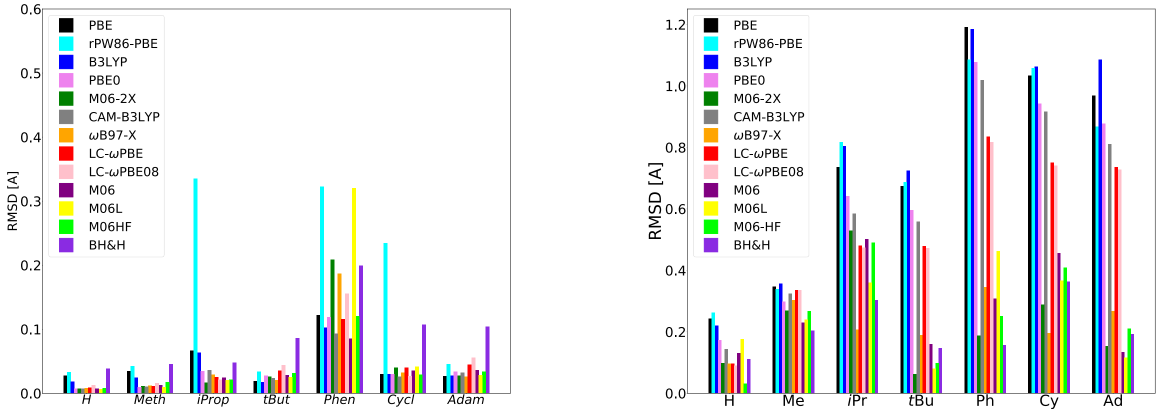

(a)

(b)

Figure S3: RMSD with hydrogens (Å) between DFAs and CC2 geometries for *trans* (left) and *cis* isomers (right), calculated using DFAs without dispersion corrections. RI-MP2 results are also shown for comparison.

Table S10: RMSD (Å) between geometries optimized using DFAs with and without dispersion corrections (in parenthesis) for E and Z isomers.

Molecule	Approx.	RMSD (E)	RMSD (Z)
a (R = H)	PBE(D3)	0.00	0.05
	rPW86PBE (VV)	0.01	0.06
	PBE0(D3)	0.00	0.05
	B3LYP(D3)	0.00	0.07
	M06-2X(D3)	0.00	0.00
	CAM-B3LYP(D3)	0.00	0.05
	LC-ωPBE(D3)	0.00	0.06
	LC-ωPBE08(VV)	0.01	0.01
	ωB97X(D)	0.00	0.02
b (R = Me)	PBE(D3)	0.00	0.01
	rPW86PBE(VV)	0.01	0.08
	PBE0(D3)	0.00	0.10
	B3LYP(D3)	0.01	0.12
	M06-2X(D3)	0.00	0.03
	CAM-B3LYP(D3)	0.00	0.10
	LC-ωPBE(D3)	0.00	0.12
	LC-ωPBE08(VV)	0.01	0.16
	ωB97X(D)	0.00	0.06
c (R = iPr)	PBE(D3)	0.01	0.72
	rPW86PBE(VV)	0.03	0.73
	PBE0(D3)	0.01	0.64
	B3LYP(D3)	0.02	0.77
	M06-2X(D3)	0.00	0.05
	CAM-B3LYP(D3)	0.02	0.62
	LC-ωPBE(D3)	0.02	0.65
	LC-ωPBE08(VV)	0.01	0.53
	ωB97X(D)	0.00	0.15

Molecule	Approx.	RMSD (E)	RMSD (Z)
d (R = tBu)	PBE(D3)	0.01	0.53
	rPW86PBE(VV)	0.02	0.59
	PBE0(D3)	0.01	0.47
	B3LYP(D3)	0.01	0.64
	M06-2X(D3)	0.00	0.05
	CAM-B3LYP(D3)	0.01	0.44
	LC-ωPBE(D3)	0.01	0.49
	LC-ωPBE08(VV)	0.01	0.49
	ωB97X(D)	0.01	0.23
e (R = Ph)	PBE(D3)	0.03	0.97
	rPW86PBE(VV)	0.02	0.74
	PBE0(D3)	0.03	0.88
	B3LYP(D3)	0.03	1.07
	M06-2X(D3)	0.04	0.05
	CAM-B3LYP(D3)	0.03	0.89
	LC-ωPBE(D3)	0.03	0.72
	LC-ωPBE08(VV)	0.03	0.71
	ωB97X(D)	0.03	0.22
f (R = Cy)	PBE(D3)	0.03	1.00
	rPW86PBE(VV)	0.03	1.08
	PBE0(D3)	0.03	0.94
	B3LYP(D3)	0.04	1.11
	M06-2X(D3)	0.01	0.04
	CAM-B3LYP(D3)	0.03	0.94
	LC-ωPBE(D3)	0.03	0.81
	LC-ωPBE08(VV)	0.03	0.76
	ωB97X(D)	0.01	0.18
g (R = Ad)	PBE(D3)	0.02	0.90
	rPW86PBE(VV)	0.02	1.15
	PBE0(D3)	0.02	0.79
	B3LYP(D3)	0.02	1.02
	M06-2X(D3)	0.00	0.07
	CAM-B3LYP(D3)	0.02	0.69
	LC-ωPBE(D3)	0.02	0.61
	LC-ωPBE08(VV)	0.02	0.61
	ωB97X(D)	0.01	0.27

Table S11: RMSD (Å) between DFAs and CC2 geometries for *E* and *Z* isomers, calculated using DFAs without and with dispersion corrections. RMSD between MP2 and CC2 geometries are also reported.

Compound	Approx.	RMSD (*E*)	RMSD (*Z*)
a (R = H)	RI-MP2	0.02	0.02
	PBE	0.03	0.24
	PBE-D3	0.03	0.20
	rPW86PBE-VV	0.03	0.21
	rPW86PBE	0.03	0.26
	PBE0	0.01	0.17
	PBE0-D3	0.01	0.13
	B3LYP	0.02	0.22
	B3LYP-D3	0.02	0.15
	CAM-B3LYP	0.01	0.14
	CAM-B3LYP-D3	0.01	0.10
	LC-ωPBE	0.01	0.10
	LC-ωPBE-D3	0.01	0.08
	LC-ωPBE08	0.01	0.09
	LC-ωPBE08-VV	0.02	0.26
	ωB97-X	0.01	0.10
	ωB97-X-D	0.01	0.08
	BH&H	0.04	0.11
	M06	0.01	0.13
	M06L	0.01	0.18
	M06-2X	0.01	0.10
	M06-2X-D3	0.01	0.09
	M06-HF	0.01	0.03

Compound	Approx.	RMSD (*E*)	RMSD (*Z*)
b (R = Me)	RI-MP2	0.03	0.08
	PBE	0.04	0.35
	PBE-D3	0.03	0.27
	rPW86PBE-VV	0.04	0.26
	rPW86PBE	0.04	0.34
	PBE0	0.01	0.30
	PBE0-D3	0.01	0.22
	B3LYP	0.02	0.36
	B3LYP-D3	0.02	0.26
	CAM-B3LYP	0.01	0.32
	CAM-B3LYP-D3	0.01	0.28
	LC-ωPBE	0.01	0.34
	LC-ωPBE-D3	0.01	0.34
	LC-ωPBE08	0.01	0.34
	LC-ωPBE08-VV	0.02	0.26
	ωB97-X	0.01	0.30
	ωB97-X-D	0.01	0.27
	BH&H	0.05	0.20
	M06	0.01	0.23
	M06L	0.01	0.24
	M06-2X	0.01	0.27
	M06-2X-D3	0.01	0.26
	M06-HF	0.02	0.27
c (R = *i*Pr)	RI-MP2	0.04	0.01
	PBE	0.07	0.74
	PBE-D3	0.06	0.22
	rPW86PBE-VV	0.32	0.26
	rPW86PBE	0.34	0.68
	PBE0	0.03	0.64
	PBE0-D3	0.02	0.20
	B3LYP	0.06	0.80
	B3LYP-D3	0.04	0.19
	CAM-B3LYP	0.04	0.58
	CAM-B3LYP-D3	0.02	0.20
	LC-ωPBE	0.03	0.48
	LC-ωPBE-D3	0.01	0.38
	LC-ωPBE08	0.02	0.47
	LC-ωPBE08-VV	0.02	0.14
	ωB97-X	0.03	0.21
	ωB97-X-D	0.03	0.14
	BH&H	0.05	0.30
	M06	0.02	0.50
	M06L	0.02	0.36
	M06-2X	0.02	0.53
	M06-2X-D3	0.02	0.25
	M06-HF	0.02	0.49

Compound	Approx.	RMSD (E)	RMSD (Z)
d (R = tBu)	RI-MP2	0.003	0.002
	PBE	0.02	0.67
	PBE-D3	0.02	0.14
	rPW86PBE-VV	0.02	0.11
	rPW86PBE	0.03	0.69
	PBE0	0.03	0.60
	PBE0-D3	0.03	0.12
	B3LYP	0.02	0.73
	B3LYP-D3	0.01	0.10
	CAM-B3LYP	0.02	0.56
	CAM-B3LYP-D3	0.02	0.15
	LC-ωPBE	0.04	0.48
	LC-ωPBE-D3	0.04	0.09
	LC-ωPBE08	0.04	0.47
	LC-ωPBE08-VV	0.05	0.09
	ωB97-X	0.02	0.19
	ωB97-X-D	0.02	0.09
	BH&H	0.09	0.15
	M06	0.03	0.16
	M06L	0.03	0.08
	M06-2X	0.03	0.06
	M06-2X-D3	0.03	0.04
	M06-HF	0.03	0.10
e (R = Ph)	RI-MP2	0.01	0.03
	PBE	0.12	1.19
	PBE-D3	0.14	0.24
	rPW86PBE-VV	0.32	0.48
	rPW86PBE	0.32	1.09
	PBE0	0.12	1.08
	PBE0-D3	0.14	0.21
	B3LYP	0.10	1.18
	B3LYP-D3	0.12	0.15
	CAM-B3LYP	0.09	1.02
	CAM-B3LYP-D3	0.12	0.21
	LC-ωPBE	0.12	0.84
	LC-ωPBE-D3	0.14	0.15
	LC-ωPBE08	0.15	0.81
	LC-ωPBE08-VV	0.16	0.13
	ωB97-X	0.19	0.35
	ωB97-X-D	0.20	0.14
	BH&H	0.20	0.16
	M06	0.09	0.31
	M06L	0.32	0.46
	M06-2X	0.21	0.19
	M06-2X-D3	0.17	0.14
	M06-HF	0.12	0.25

Compound	Approx.	RMSD (E)	RMSD (Z)
f (R = Cy)	RI-MP2	0.04	0.01
	PBE	0.03	1.03
	PBE-D3	0.03	0.20
	rPW86PBE-VV	0.22	0.13
	rPW86PBE	0.23	1.06
	PBE0	0.03	0.94
	PBE0-D3	0.04	0.16
	B3LYP	0.03	1.06
	B3LYP-D3	0.03	0.16
	CAM-B3LYP	0.03	0.92
	CAM-B3LYP-D3	0.04	0.18
	LC-ωPBE	0.04	0.75
	LC-ωPBE-D3	0.06	0.15
	LC-ωPBE08	0.03	0.74
	LC-ωPBE08-VV	0.05	0.13
	ωB97-X	0.03	0.20
	ωB97-X-D	0.04	0.24
	BH&H	0.11	0.36
	M06	0.04	0.46
	M06L	0.04	0.37
	M06-2X	0.04	0.29
	M06-2X-D3	0.05	0.29
	M06-HF	0.03	0.41
g (R = Ad)	RI-MP2	0.02	0.03
	PBE	0.03	0.97
	PBE-D3	0.02	0.43
	rPw86PBE-VV	0.04	0.27
	rPw86PBE	0.05	0.87
	PBE0	0.03	0.88
	PBE0-D3	0.03	0.43
	B3LYP	0.03	1.09
	B3LYP-D3	0.02	0.42
	CAM-B3LYP	0.03	0.81
	CAM-B3LYP-D3	0.03	0.43
	LC-ωPBE	0.04	0.74
	LC-ωPBE-D3	0.04	0.42
	LC-ωPBE08	0.06	0.73
	LC-ωPBE08-VV	0.06	0.44
	wB97-X	0.03	0.27
	wB97-X-D	0.02	0.06
	BH&H	0.10	0.19
	M06	0.04	0.13
	M06L	0.03	0.12
	M06-2X	0.03	0.15
	M06-2X-D3	0.03	0.10
	M06-HF	0.03	0.21

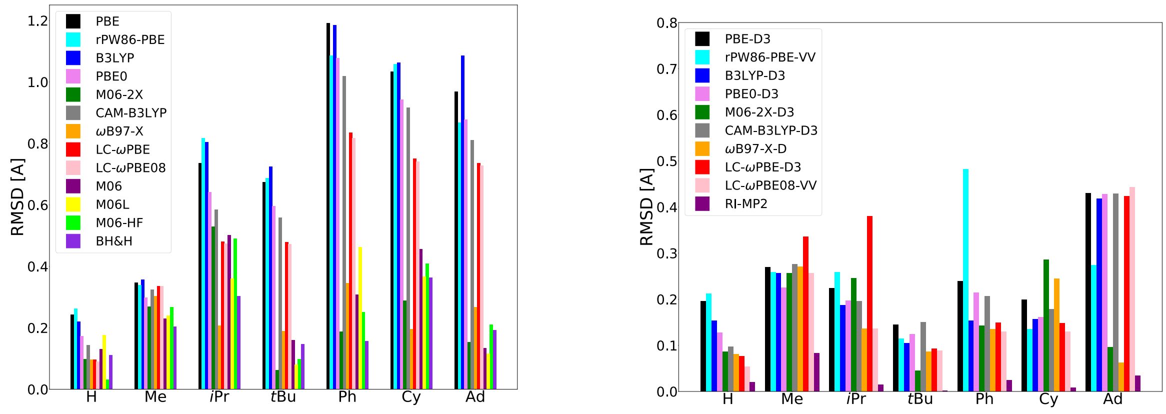

(a) (b)

Figure S4: RMSD between DFAs and CC2 geometries for *cis* isomers, calculated using DFAs without (left) and with (right) dispersion corrections. RI-MP2 results are also shown for comparison.

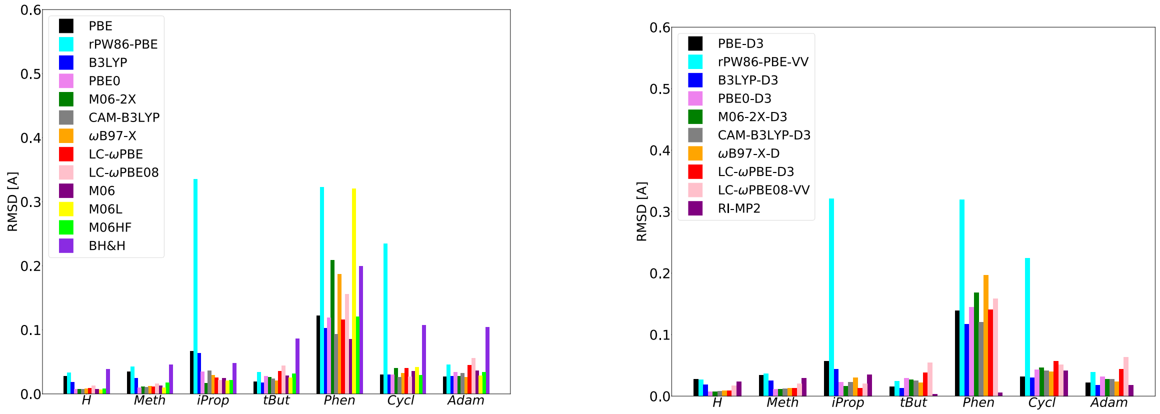

(a) (b)

Figure S5: RMSD between DFAs and CC2 geometries for *trans* isomers, calculated using DFAs without (left) and with (right) dispersion corrections. RI-MP2 results are also shown for comparison.

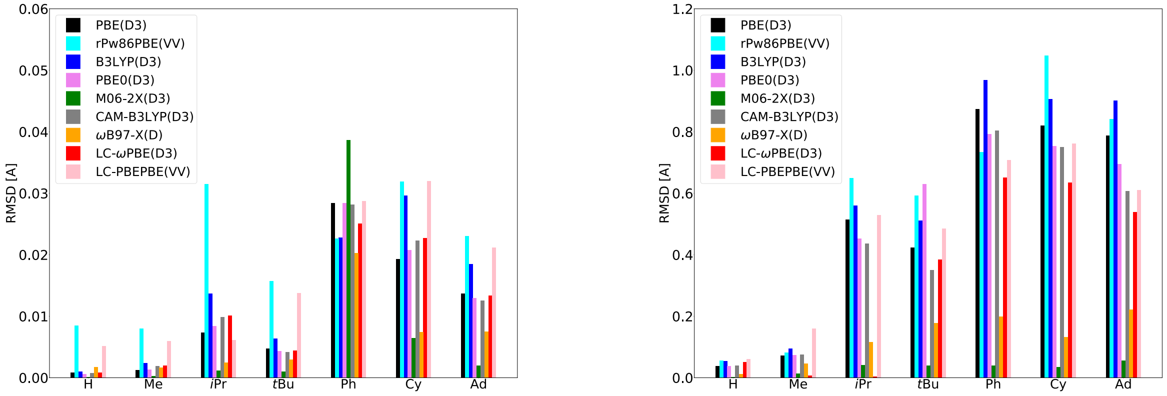

(a) (b)

Figure S6: RMSD (Å) excluding hydrogen atoms between geometries optimized using DFAs with and without dispersion corrections for *trans* (left) and *cis* (right) isomers.

8 Relative *Z*-*E* energies

8.1 CC2 *vs* MP2

Table S12: Difference in the energy of the *trans* (E) and *cis* (Z) forms, $\Delta E_{EZ} = E_Z - E_E$, as calculated at the HF, RI-CC2 and RI-MP2 levels with the cc-pVDZ basis set. All energy values are in kcal.mol^{-1}.

Molecule	Approx.	ΔE_{EZ}
a (R = H)	RI-CC2	11.46
	RI-MP2	12.01
	HF	17.9
b (R = Me)	RI-CC2	10.87
	RI-MP2	11.43
	HF	17.4
c (R = *i*Pr)	RI-CC2	8.06
	RI-MP2	8.90
	HF	17.5
d (R = *t*Bu)	RI-CC2	6.73
	RI-MP2	7.70
	HF	17.7
e (R = Ph)	RI-CC2	4.04
	RI-MP2	4.9
	HF	17.4
f (R = Cy)	RI-CC2	5.16
	RI-MP2	6.41
	HF	17.3
g (R = Ad)	RI-CC2	0.80
	RI-MP2	2.67
	HF	17.4

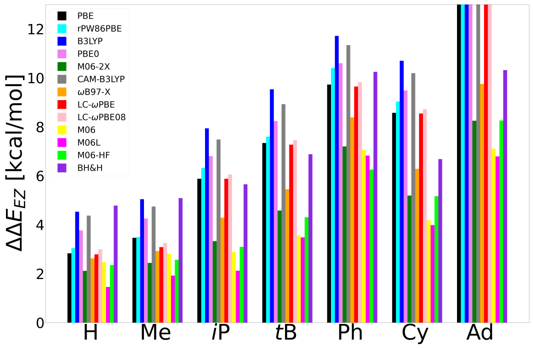

(a)

Figure S7: *Z*-*E* energy differences calculated at the CC2 level and DFAs without dispersion corrections ($\Delta\Delta E_{ZE} = \Delta E_{ZE}(DFT) - \Delta E_{ZE}(CC2)$, in kcal/mol).

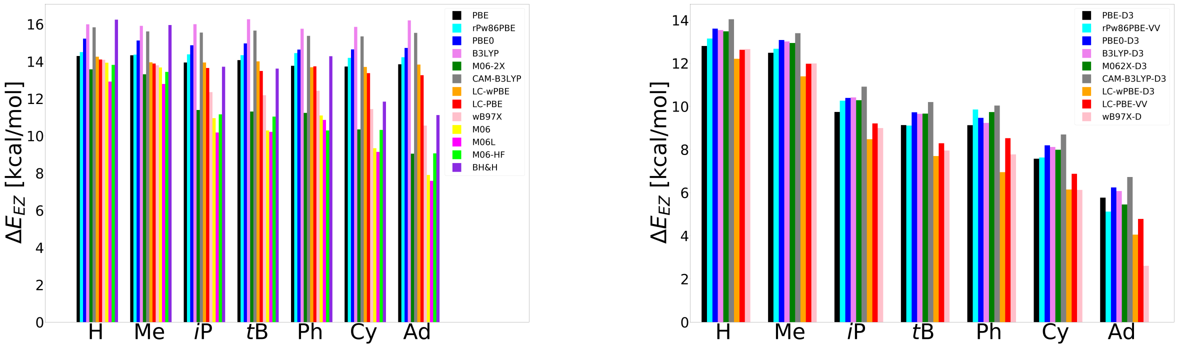

(a) (b)

Figure S8: Difference in the energy of the *trans* (E) and *cis* (Z) forms, $\Delta E_{EZ} = E_Z - E_E$, as calculated using DFAs without (left) and with (right) dispersion corrections and the cc-pVDZ basis set.

8.2 DFT relative *Z*-*E* energies

Table S13: Relative electronic energies of the E and Z conformers, $\Delta E_{ZE} = E_E - E_Z$, and relative Gibbs free energies ($\Delta G_{ZE} = G_E - G_Z$), calculated at T = 300 K and P = 1 atm. All calculations were done using the cc-pVDZ basis set. All energy values are in kcal.mol^{-1}. The Gibbs free energy have been calculated for the functionals implemented in Gaussian using the quasi-harmonic approximation (qa-G) employing the software goodvibes.py.[S15] The vibrational entropy was tested using the Grimme scheme,[S16] while the enthalpy contributions were evaluated with the Head-Gordon scheme.[S17] The threshold for which the qa-G was employed is 100 cm^{-1}. For the functionals calculated with Q-Chem (namely, rPW86-PBE, rPW86-PBE-VV, LC-ωPBE08 and LC-ωPBE08-VV) frequency calculations do not have been performed because analytical calculations are not implemented, and therefore free energies are not available. For RI-CC2 and RI-MP2 the Gibbs free energies correspond to normal computations.

Compound	Approx.	ΔE_{ZE}	ΔG_{ZE}
a (R = H)	RI-CC2	-11.5	-11.6
	RI-MP2	-12.0	-12.3
	PBE	-14.3	-13.6
	PBE-D3	-12.8	-12.2
	PBE0	-15.2	-14.7
	PBE0-D3	-13.6	-13.1
	rPW86-PBE	-14.5	
	rPW86-PBE-VV	-13.1	
	B3LYP	-16.0	-15.4
	B3LYP-D3	-13.5	-13.0
	BH&H	-16.2	-15.7
	CAM-B3LYP	-15.8	-15.3
	CAM-B3LYP-D3	-14.0	-13.6
	ωB97-X	-14.1	-13.7
	ωB97-X-D	-12.7	-12.4
	LC-ωPBE	-14.2	-14.0
	LC-ωPBE-D3	-12.2	-12.1
	LC-ωPBE08	-14.5	
	LC-ωPBE08-VV	-12.8	
	M06	-13.9	-13.5
	M06L	-12.9	-12.4
	M06-2X	-13.6	-13.1
	M06-2X-D3	-13.5	-12.8
	M06-HF	-13.8	-13.4
	HF	-17.9	-17.5

Compound	Approx.	ΔE_{ZE}	ΔG_{ZE}
b (R = Me)	RI-CC2	-10.9	-11.4
	RI-MP2	-11.4	-12.1
	PBE	-14.3	-13.5
	PBE-D3	-12.5	-11.9
	PBE0	-15.1	-14.7
	PBE0-D3	-13.1	-12.7
	rPW86-PBE	-14.4	
	rPW86-PBE-VV	-12.7	
	B3LYP	-15.9	-15.4
	B3LYP-D3	-13.0	-12.7
	BH&H	-16.0	-15.2
	CAM-B3LYP	-15.6	-15.3
	CAM-B3LYP-D3	-13.4	-13.2
	ωB97-X	-13.8	-13.7
	ωB97-X-D	-12.0	-11.4
	LC-ωPBE	-14.0	-14.0
	LC-ωPBE-D3	-11.4	-11.5
	LC-ωPBE08	-14.1	
	LC-ωPBE08-VV	-12.1	
	M06	-13.6	-13.8
	M06L	-12.8	-12.3
	M06-2X	-13.3	-13.7
	M06-2X-D3	-12.9	-13.2
	M06-HF	-13.4	-13.9
	HF	-17.4	-17.2

Compound	Approx.	ΔE_{ZE}	ΔG_{ZE}
c (R = iPr)	RI-CC2	-8.1	-8.4
	RI-MP2	-8.9	-9.5
	PBE	-13.9	-14.1
	PBE-D3	-9.7	-10.5
	PBE0	-14.9	-15.1
	PBE0-D3	-10.4	-11.1
	rPW86-PBE	-14.4	
	rPW86-PBE-VV	-10.3	
	B3LYP	-16.0	-16.1
	B3LYP-D3	-10.4	-11.5
	BH&H	-13.7	-14.5
	CAM-B3LYP	-15.5	-15.7
	CAM-B3LYP-D3	-10.9	-11.8
	ωB97-X	-12.3	-13.6
	ωB97-X-D	-9.0	-10.1
	LC-ωPBE	-13.9	-14.6
	LC-ωPBE-D3	-8.5	-10.2
	LC-ωPBE08	-14.1	
	LC-ωPBE08-VV	-9.2	
	M06	-11.0	-13.0
	M06L	-10.2	-11.3
	M06-2X	-11.4	-12.6
	M06-2X-D3	-10.3	-11.4
	M06-HF	-11.2	-14.0
	HF	-17.5	-17.7

Compound	Approx.	ΔE_{ZE}	ΔG_{ZE}
d (R = *t*Bu)	RI-CC2	-6.7	-7.5
	RI-MP2	-7.7	-8.6
	PBE	-14.1	-13.9
	PBE-D3	-9.1	-9.5
	PBE0	-15.0	-15.0
	PBE0-D3	-9.7	-10.3
	rPW86-PBE	-14.3	
	rPW86-PBE-VV	-9.1	
	B3LYP	-16.3	-16.2
	B3LYP-D3	-9.7	-10.5
	BH&H	-13.6	-14.2
	CAM-B3LYP	-15.7	-15.8
	CAM-B3LYP-D3	-10.2	-11.0
	ωB97-X	-12.2	-13.0
	ωB97-X-D	-8.0	-9.9
	LC-ωPBE	-14.0	-14.4
	LC-ωPBE-D3	-7.7	-8.8
	LC-ωPBE08	-14.2	
	LC-ωPBE08-VV	-8.2	
	M06	-10.3	-11.5
	M06L	-10.2	-11.6
	M06-2X	-11.3	-11.9
	M06-2X-D3	-9.7	-10.2
	M06-HF	-11.0	-11.6
	HF	-17.7	-18.0

Compound	Approx.	ΔE_{ZE}	ΔG_{ZE}
e (R = Ph)	RI-CC2	-4.0	-5.9
	RI-MP2	-4.9	-7.0
	PBE	-13.8	-13.3
	PBE-D3	-9.1	-9.3
	PBE0	-14.6	-14.3
	PBE0-D3	-9.5	-9.7
	rPW86-PBE	-14.4	
	rPW86-PBE-VV	-9.9	
	B3LYP	-15.8	-15.3
	B3LYP-D3	-9.2	-10.0
	BH&H	-14.3	-14.4
	CAM-B3LYP	-15.4	-15.0
	CAM-B3LYP-D3	-10.0	-10.7
	ωB97-X	-12.4	-12.4
	ωB97-X-D	-7.8	-8.5
	LC-ωPBE	-13.7	-13.5
	LC-ωPBE-D3	-7.0	-8.0
	LC-ωPBE08	-13.9	
	LC-ωPBE08-VV	-7.9	
	M06	-11.1	-11.6
	M06L	-10.9	-10.9
	M06-2X	-11.2	-11.0
	M06-2X-D3	-9.7	-9.9
	M06-HF	-10.3	-10.5
	HF	-17.4	-17.2

Compound	Approx.	ΔE_{ZE}	ΔG_{ZE}
f (R = Cy)	RI-CC2	-5.2	-5.5
	RI-MP2	-6.4	-7.0
	PBE	-13.7	-13.5
	PBE-D3	-7.6	-8.6
	PBE0	-14.6	-14.4
	PBE0-D3	-8.2	-9.4
	rPW86-PBE	-14.2	
	rPW86-PBE-VV	-7.6	
	B3LYP	-15.9	-15.8
	B3LYP-D3	-8.1	-9.7
	BH&H	-11.8	-13.2
	CAM-B3LYP	-15.3	-15.3
	CAM-B3LYP-D3	-8.7	-10.3
	ωB97-X	-11.4	-12.5
	ωB97-X-D	-6.1	-8.2
	LC-ωPBE	-13.7	-13.8
	LC-ωPBE-D3	-6.1	-7.9
	LC-ωPBE08	-13.9	
	LC-ωPBE08-VV	-6.8	
	M06	-9.3	-10.1
	M06L	-9.1	9.0
	M06-2X	-10.3	-11.5
	M06-2X-D3	-8.0	-9.5
	M06-HF	-10.3	-12.2
	HF	-17.3	-17.5

Compound	Approx.	ΔE_{ZE}	ΔG_{ZE}
g (R = Ad)	RI-CC2	-0.8	
	RI-MP2	-2.7	-4.9
	PBE	-13.8	-13.7
	PBE-D3	-5.8	-6.9
	PBE0	-14.7	-14.5
	PBE0-D3	-6.2	-7.5
	rPW86-PBE	-14.2	
	rPW86-PBE-VV	-5.1	
	B3LYP	-16.2	-15.7
	B3LYP-D3	-6.1	-7.7
	BH&H	-11.1	-12.4
	CAM-B3LYP	-15.5	-14.7
	CAM-B3LYP-D3	-6.7	-8.3
	ωB97-X	-10.6	-12.1
	ωB97-X-D	-2.6	-3.7
	LC-ωPBE	-13.8	-13.9
	LC-ωPBE-D3	-4.1	-6.2
	LC-ωPBE08	-14.0	
	LC-ωPBE08-VV	-4.2	
	M06	-7.9	8.2
	M06L	-7.6	-9.1
	M06-2X	-9.0	-10.4
	M06-2X-D3	-5.5	-6.8
	M06-HF	-9.1	-10.4
	HF	-17.4	-17.8

9 Calculations for the Ph molecule

DFAs with dispersion corrections are able to reproduce qualitatively well the energy gap of all the systems considered. However, we observed that are much less accurate for the compound **f**, which includes phenyl substituents in the *meso* position. In order to investigate these discrepancies, we performed single-point calculations on the RI-CC2 geometries for this molecule. The results are collected in Table S14 and Fig. S9.

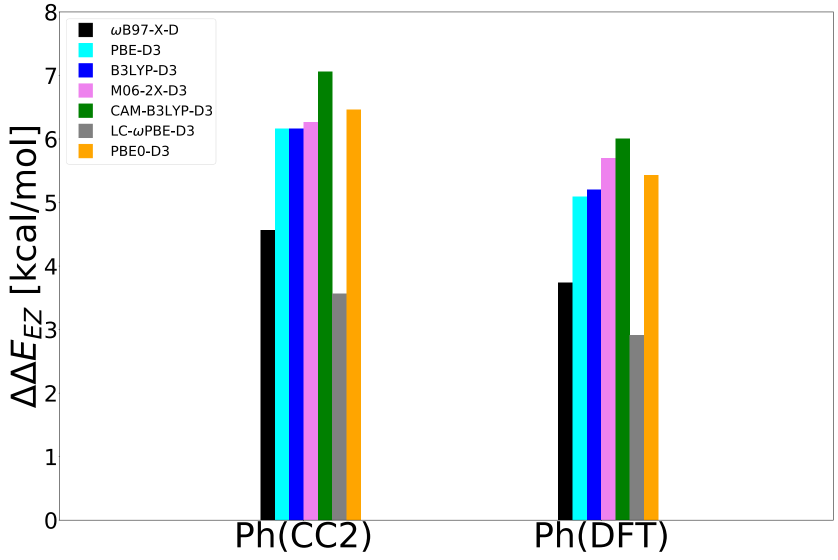

Figure S9: $Z - E$ energy differences with respect to RI-CC2 issued from DFAs for the molecule with R = Ph, using reference RI-CC2 geometries (left) and optimized DFAs geometries (right) with dispersion corrections ($\Delta\Delta E_{ZE} = \Delta E^{DFT}_{ZE}(DFT/CC2)\ \Delta E^{CC2}_{ZE}(CC2)$, in kcal/mol).

Table S14: $Z - E$ energy differences issued from RI-CC2 and DFAs for the molecule with R = Ph, using reference RI-CC2 geometries (left) and optimized DFAs' geometries (right) with dispersion corrections (in kcal/mol).

Compound	Approx.	$\Delta E_{EZ}(RI - CC2)$	$\Delta E_{EZ}(DFT)$
Ph	RI-CC2	-4.0	-
	ωB97-X-D	-8.6	-7.8
	PBE-D3	-10.2	-9.1
	PBE0-D3	-10.5	-9.5
	B3LYP-D3	-10.2	-9.2
	M06-2X-D3	-10.3	-9.7
	CAM-B3LYP-D3	-11.1	-10.0
	LC-ωPBE-D3	-7.6	-6.9

10 Nonlinear Optical properties

10.1 Reference RI-MP2 results

The accuracy of the RI approximation in the evaluation of β has been tested for the molecule R=H, with respect to the standard MP2 calculation.

Molecule	β_{MP2}	β_{RI-MP2}
R= H	52.55	52.52

10.2 *ab initio* results

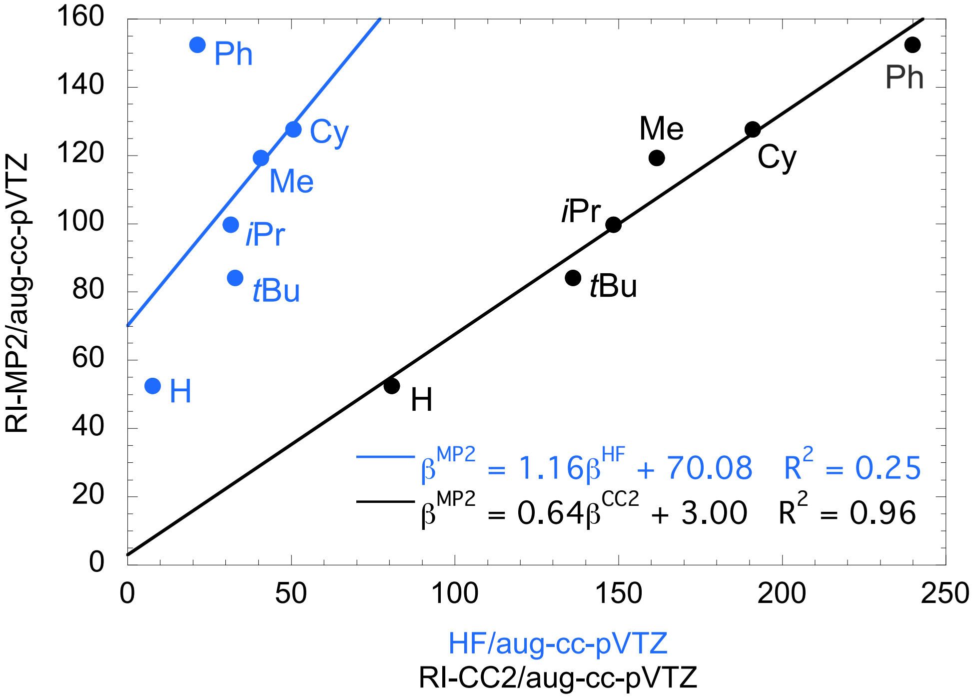

Figure S10: Correlation between static hyperpolarizabilities (a.u.) of the series of azobenzenes calculated at the MP2 level with respect to the values calculated using CC2 and HF.

10.3 DFT results

Table S15: Total first hyperpolarizabilities (β, a.u.) of the *cis* isomers, calculated using various levels of approximation with the aug-cc-pVTZ basis set, using RI-CC2/cc-pVDZ geometries.

Compound	Approx.	β
a (R = H)	RI-MP2	52.5
	RI-CC2	80.8
	PBE	99.6
	rPW86-PBE	107.2
	rPW86-PBE-VV	104.0
	PBE0	73.1
	B3LYP	83.3
	BH&H	41.1
	CAM-B3LYP	52.4
	ωB97X	44.0
	ωB97X-D	61.5
	LC-BLYP	22.2
	Tα-LC-BLYP	44.3
	LC-PBE	23.6
	LC-ωPBE	31.2
	LC-PBE-VV	42.5
	M06	96.8
	M06L	136.3
	M06-2X	43.8
	M06-HF	1.5
	HF	7.7
b (R = Me)	RI-MP2	119.3
	RI-CC2	161.7
	PBE	186.6
	rPW86-PBE	196.4
	rPW86-PBE-VV	200.4
	PBE0	142.8
	B3LYP	155.8
	BH&H	99.3
	CAM-B3LYP	115.4
	ωB97X	107.2
	ωB97X-D	132.0
	LC-BLYP	75.6
	Tα-LC-BLYP	109.6
	LC-PBE	76.6
	LC-ωPBE	87.5
	LC-PBE-VV	85.5
	M06	166.0
	M06L	227.1
	M06-2X	100.0
	M06-HF	46.7
	HF	40.7

Compound	Approx.	β
c (R = iPr)	RI-MP2	99.8
	RI-CC2	148.5
	PBE	176.1
	rPW86-PBE	183.9
	rPW86-PBE-VV	186.0
	PBE0	117.3
	B3LYP	132.7
	BH&H	71.6
	CAM-B3LYP	92.7
	ωB97X	76.8
	ωB97X-D	95.4
	LC-BLYP	56.7
	Tα-LC-BLYP	86.1
	LC-PBE	55.3
	LC-ωPBE	66.9
	LC-PBE-VV	58.9
	M06	150.4
	M06L	196.5
	M06-2X	84.8
	M06-HF	46.3
	HF	31.6
d (R = tBu)	RI-MP2	84.1
	RI-CC2	136.1
	PBE	179.2
	rPW86-PBE	188.2
	rPW86-PBE-VV	187.5
	PBE0	115.5
	B3LYP	130.8
	BH&H	68.3
	CAM-B3LYP	91.3
	ωB97X	83.2
	ωB97X-D	107.1
	LC-BLYP	58.4
	Tα-LC-BLYP	84.9
	LC-PBE	56.4
	LC-ωPBE	67.5
	LC-PBE-VV	70.4
	M06	159.5
	M06L	218.0
	M06-2X	81.6
	M06-HF	41.6
	HF	32.9

Compound	Approx.	β
e (R = Ph)	RI-MP2	152.4
	RI-CC2	239.8
	PBE	266.2
	rPW86-PBE	253.3
	rPW86-PBE-VV	294.2
	PBE0	158.3
	B3LYP	174.7
	BH&H	100.2
	CAM-B3LYP	99.7
	ωB97X	84.4
	ωB97X-D	107.6
	LC-BLYP	53.9
	Tα-LC-BLYP	85.0
	LC-PBE	59.5
	LC-ωPBE	66.7
	LC-PBE-VV	72.8
	M06	207.8
	M06L	277.9
	M06-2X	115.9
	M06-HF	36.4
	HF	21.3
f (R = Cy)	RI-MP2	127.7
	RI-CC2	191.0
	PBE	294.3
	rPW86-PBE	348
	rPW86-PBE-VV	253.7
	PBE0	158.0
	B3LYP	175.3
	BH&H	97.8
	CAM-B3LYP	119.2
	ωB97X	105.1
	ωB97X-D	131.0
	LC-BLYP	75.7
	Tα-LC-BLYP	107.2
	LC-PBE	75.7
	LC-ωPBE	88.4
	LC-PBE-VV	79.3
	M06	202.3
	M06L	263.4
	M06-2X	111.6
	M06-HF	59.1
	HF	50.1

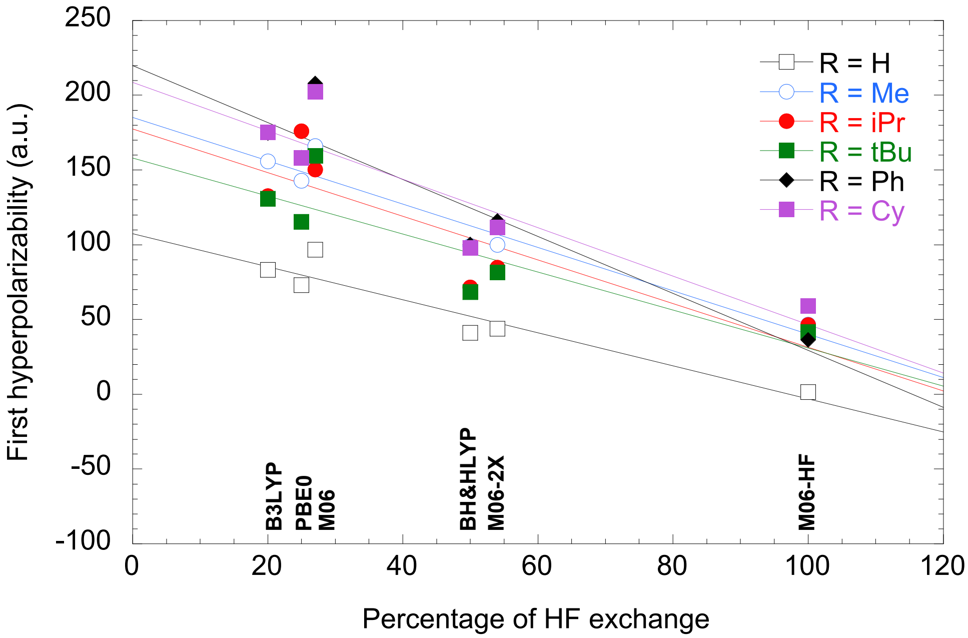

Figure S11: Evolution of the static hyperpolarizabilities (a.u.) of the series of azobenzenes calculated using various DFAs in combination with the aug-cc-pVTZ basis set, as a function of the percentage of exact Hartree-Fock exchange.

Table S16: Absolute errors relative to MP2 (AE(%) = $|\beta_{DFT} - \beta_{MP2}|/\beta_{MP2} \times 100$) on the total first hyperpolarizabilities of *cis* isomers, as calculated for selected hybrid functionals.

DFA	R = H	R = Me	R = *i*Pr	R = *t*Bu	R = Ph	R = Cy	Mean AE
PBE0	52.4	38.7	43.1	109.4	24.2	23.7	48.6
B3LYP	61.9	30.2	56.1	57.8	14.2	44.0	37.3
BH&H	4.8	65.5	0.5	14.9	55.2	23.4	27.4
M06	48.6	18.9	66.3	78.8	4.7	58.4	46.0
M06-2X	2.9	63.3	0.2	0.8	46.5	12.6	21.0
M06-HF	90.5	98.7	53.2	44.9	72.7	53.7	69.0
best DFA	M06-2X	M06	M06-2X	M06-2X	M06	M06-2X	M06-2X

Table S17: Absolute errors relative to MP2 (AE(%) = $|\beta_{DFT} - \beta_{MP2}|/\beta_{MP2} \times 100$) on the total first hyperpolarizabilities of *cis* isomers, as calculated for selected hybrid range-separated functionals.

DFA	R = H	R = Me	R = *i*Pr	R = *t*Bu	R = Ph	R = Cy	Mean AE
CAM-B3LYP	0.2	3.3	7.1	8.6	34.6	6.7	10.1
LC-BLYP	57.7	36.6	43.2	30.6	64.6	40.7	45.6
LC-PBE	55.0	35.8	44.6	32.9	61.0	40.7	45.0
LC-ωPBE	40.6	26.7	33.0	19.7	56.2	30.8	34.5
ωB97X	16.2	10.1	23.0	1.1	44.6	17.7	18.8
ωB97X-D	17.1	10.6	4.4	27.3	29.4	2.6	15.3
best DFA	CAM	CAM	ωB97X-D	ωB97X	ωB97X-D	ωB97X-D	CAM

11 PNOC analysis

Table S18: Vector (β_i) and tensor (β_{ijk}) components of the total first hyperpolarizability, as calculated summing all the orbital contributions of the hyperpolarizzability tensors obtained by the PNOC analysis at CAM-B3LYP/6-311++G** level.

Molecule	β_{xxx}	β_{yyx}	β_{zzx}	β_x	β_{yyy}	β_{xxy}	β_{zzy}	β_y	β_{zzz}	β_{xxz}	β_{yyz}	β_z	β_{tot}
a (R = **H**)	-0.0	-0.1	0.0	-0.4	2.9	-10.4	0.1	-22.3	31.4	-155.9	14.5	-330.2	66.2
b (R = **Me**)	-0.4	-2.2	1.9	-2.1	4.2	8.3	-1.1	34.3	-30.7	-160.7	-26.7	-654.4	131.1
c (R = ***i*Pr**)	-2.3	-0.9	0.6	-7.9	-16.0	8.6	8.2	2.0	-15.6	-145.6	17.7	-430.6	86.1
d (R = ***t*Bu**)	-32.2	10.1	-9.5	-94.9	-3.0	0.5	18.4	47.8	-21.7	-170.2	52.4	-418.5	86.3
e (R = **Ph**)	-0.3	-6.3	5.9	-1.9	13.7	6.6	-10.2	30.3	22.7	-148.1	-98.6	-672.3	134.6
f (R = **Cy**)	5.4	6.0	-12.1	-2.2	7.7	5.4	-1.7	34.2	-13.5	-142.5	-39.9	-587.8	117.8
g (R = **Ad**)	2.7	-22.4	14.3	-15.9	-54.3	-18.5	4.1	-206.0	-70.2	-170.0	4.2	-708.0	147.5

Table S19: Vector (β_i) and tensor (β_{ijk}) components of the total first hyperpolarizability, as calculated through the CPKS method at CAM-B3LYP/6-311++G** level.

Molecule	β_{xxx}	β_{yyx}	β_{zzx}	β_x	β_{yyy}	β_{xxy}	β_{zzy}	β_y	β_{zzz}	β_{xxz}	β_{yyz}	β_z	β_{tot}
a (R = **H**)	0.0	0.0	0.1	0.2	2.8	-10.5	0.2	-22.4	31.3	-155.9	14.4	-330.3	66.2
b (R = **Me**)	0.1	-2.0	2.1	0.8	4.1	8.3	-1.1	33.6	-30.2	-160.5	-26.5	-651.5	130.5
c (R = ***i*P**)	-1.8	-0.7	0.7	-5.4	-16.4	8.5	8.2	0.8	-15.3	-145.7	18.1	-428.8	85.8
d (R = ***t*Bu**)	-31.7	10.1	-9.4	-92.7	-3.2	0.7	18.6	48.4	-21.8	-170.3	52.3	-419.7	86.5
e (R = **Ph**)	0.1	-6.1	6.0	0.1	13.7	6.7	-10.3	30.3	23.1	-148.3	-98.5	-671.2	134.4
f (R = **Cy**)	6.0	6.3	12.1	73.4	8.3	5.4	-1.5	36.6	-12.9	-142.2	-39.2	-582.9	117.7
g (R = **Ad**)	0.8	-22.6	16.6	-16.6	-55.7	-8.3	8.7	-166.1	-68.0	-170.4	0.6	-713.3	146.5

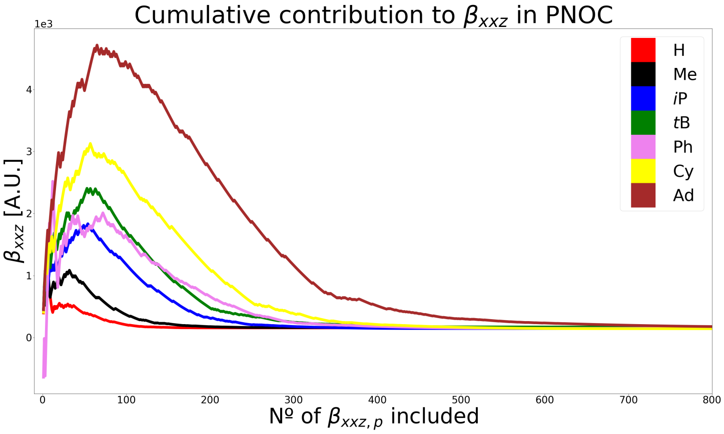

Figure S12: Accumulation of the first most important 800 orbital contributions of $\beta_{xyz,p}$ for the azobenzene derivatives. The index p indicates the corresponding orbital that is included.

Table S20: Predominant orbitals and corresponding hyperpolarizability contribution according to PNOC decomposition, ordered by importance. Units are a.u. Calculations done with CAM-B3LYP functional for the azobenzene series. H and L indicate the HOMO and LUMO for each compound. N_H is the total number of occupied MOs.

R=H N_H=48

N_{orb}	β_{zxx}	N_{orb}	β_{zyy}	N_{orb}	β_{zzz}
H	397.0	H-1	137.0	H-3	182.5
H-3	268.5	L+2	-127.4	H-2	181.2
H-2	261.6	H-3	118.7	L+3	-169.9
H-4	240.2	H-2	109.9	L+7	-114.3
L+3	-200.2	L+3	-94.7	L+1	-103.7
L+8	-193.5	H	79.6	H-1	100.4

R=Me N_H=64

N_{orb}	β_{zxx}	N_{orb}	β_{zyy}	N_{orb}	β_{zzz}
H	464.7	H-1	204.5	H-3	221.8
H-3	356.5	H-2	181.5	H-2	212.8
L+4	-300.3	L+2	-149.0	L+4	-156.9
H-2	268.7	L+7	-146.2	H-1	152.6
L+2	-244.7	H-3	142.2	L+2	-145.4
H-1	224.3	H	122.5	L+7	-132.5

R=iPr N_H=96

N_{orb}	β_{zxx}	N_{orb}	β_{zyy}	N_{orb}	β_{zzz}
H	410.9	H-1	263.8	H-3	216.7
H-3	337.4	H-2	215.0	H-2	187.9
H-2	246.0	L+4	-199.6	H-1	143.0
L+5	-231.1	H-3	182.8	L+5	-113.2
H-1	184.5	H-5	157.4	L+8	-111.0
L+6	-181.5	H	148.4	L+4	-107.4

R=tBu N_H=112

N_{orb}	β_{zxx}	N_{orb}	β_{zyy}	N_{orb}	β_{zzz}
H	459.0	H-1	253.9	H-3	222.5
H-3	381.5	H-2	203.2	H-2	209.7
H-2	239.9	H-5	163.5	L+6	-151.8
L+5	-219.2	H-4	162.9	H-1	141.6
H-1	190.5	H	143.0	L+5	-134.6
105	186.9	L+4	-138.1	L+1	-100.8

R=Ph N_H=128

N_{orb}	β_{zxx}	N_{orb}	β_{zyy}	N_{orb}	β_{zzz}
L+2	-638.7	H-1	1030.9	H-1	631.0
H-3	624.6	H-2	997.7	H-2	533.1
L+1	-605.1	L+2	-953.8	L+2	-451.5
H-1	528.4	H-3	942.6	L+3	-434.8
H-2	505.2	L+3	-862.9	H+2	-285.8
H-5	494.8	H+2	-860.3	H-6	272.5

R=Cy N_H=140

N_{orb}	β_{zxx}	N_{orb}	β_{zyy}	N_{orb}	β_{zzz}
H	408.4	H-1	327.0	H-3	214.1
H-3	332.7	H-2	286.2	H-2	193.2
H-2	265.1	H-3	224.2	H-1	158.6
H-1	207.8	H-5	213.8	L+5	-151.1
L+5	-185.3	H-16	198.8	H-16	149.2
H-7	169.9	L+5	-197.4	H-13	148.8

R=Ad N_H=196

N_{orb}	β_{zxx}	N_{orb}	β_{zyy}	N_{orb}	β_{zzz}
H	448.86	H-1	330.88	H-3	229.41
H-3	352.31	H-2	287.14	H-2	205.59
H-2	265.25	H-3	208.47	H-1	175.41
H-1	235.28	H-5	207.32	H-9	158.35
H-6	224.77	H	189.34	H-12	157.32
H-7	205.63	H-7	184.2	H-15	134.75

Table S21: Comparison between the predominant orbital contribution of the hyperpolarizability (in a. u.) tested for the functionals CAM-B3LYP and PBE performed on the substituents R=*i*Pr and R=Ph. *H* indicates the number of the HOMO orbital for each compound while *L* indicates the corresponding LUMO.

R=iP N_H=96

CAM-B3LYP		PBE	
N_{orb}	β_{zxx}	N_{orb}	β_{zxx}
H	410.9	H-3	561.7
H-3	337.4	H-4	514.8
H-2	246.0	L+3	-405.5
L+4	-231.1	L+2	-357.6
H-1	184.5	L+1	-335.4
L+5	-181.5	H	268.4

R=Ph N_H=128

CAM-B3LYP		PBE	
N_{orb}	β_{zxx}	N_{orb}	β_{zxx}
L+2	-638.7	L+2	-918.82
H-3	624.6	H-3	862.83
L+1	-605.1	L+1	-795.17
H-1	528.4	H-2	685.38
H-2	505.2	H-4	608.30
H-5	494.8	H-1	593.97

References

(S1) Gould, T. ‘Diet GMTKN55’ offers accelerated benchmarking through a representative subset approach. *Phys. Chem. Chem. Phys.* **2018**, *20*, 27735–27739.

(S2) Perdew, J. P.; Burke, K.; Ernzerhof, M. Generalized Gradient Approximation Made Simple. *Phys. Rev. Lett.* **1996**, *77*, 3865–3868.

(S3) Zhao, Y.; Truhlar, D. G. The M06 Suite of Density Functionals for Main Group Thermochemistry, Thermochemical Kinetics, Noncovalent Interactions, Excited States, and Transition Elements: two New Functionals and Systematic Testing of Four M06-Class Functionals and 12 Other Functionals. *Theor. Chem. Acc.* **2008**, *120*, 215–241.

(S4) Vydrov, O. A.; Van Voorhis, T. Nonlocal van der Waals density functional: The simpler the better. **2010**, *133*, 244103.

(S5) Stephens, P. J.; Devlin, F. J.; Chabalowski, C. F.; Frisch, M. J. Ab Initio Calculation of Vibrational Absorption and Circular Dichroism Spectra Using Density Functional Force Fields. *The Journal of Physical Chemistry* **1994**, *98*, 11623–11627.

(S6) Perdew, J. P.; Burke, K.; Ernzerhof, M. Generalized Gradient Approximation Made Simple. *Phys. Rev. Lett.* **1996**, *77*, 3865–3868.

(S7) Becke, A. D. A new mixing of Hartree–Fock and local density-functional theories. *The Journal of Chemical Physics* **1993**, *98*, 1372–1377.

(S8) Yanai, T.; Tew, D. P.; Handy, N. C. A new hybrid exchange–correlation functional using the Coulomb-attenuating method (CAM-B3LYP). *Chem. Phys. Lett.* **2004**, *393*, 51 – 57.

(S9) Vydrov, O. A.; Scuseria, G. E. Assessment of a long-range corrected hybrid functional. *The Journal of Chemical Physics* **2006**, *125*, 234109.

(S10) Iikura, H.; Tsuneda, T.; Yanai, T.; Hirao, K. A long-range correction scheme for generalized-gradient-approximation exchange functionals. *The Journal of Chemical Physics* **2001**, *115*, 3540–3544.

(S11) Besalú-Sala, P.; Sitkiewicz, S. P.; Salvador, P.; Matito, E.; Luis, J. M. A new tuned range-separated density functional for the accurate calculation of second hyperpolarizabilities. *Phys. Chem. Chem. Phys.* **2020**, *22*, 11871–11880.

(S12) Chai, J.-D.; Head-Gordon, M. Systematic optimization of long-range corrected hybrid density functionals. *The Journal of Chemical Physics* **2008**, *128*, 084106.

(S13) Chai, J.-D.; Head-Gordon, M. Long-range corrected hybrid density functionals with damped atom–atom dispersion corrections. *Phys. Chem. Chem. Phys.* **2008**, *10*, 6615–6620.

(S14) Sitkiewicz, S.; Ramos-Cordoba, E.; Luis, J. M.; Matito, E. How Many Electrons Does a Molecular Electride Hold? *J. Phys. Chem. A* **doi:10.1021/acs.jpca.1c02760**, accepted.

(S15) Luchini, G.; Alegre-Requena, J.; Funes-Ardoiz, I.; Paton, R. GoodVibes: automated thermochemistry for heterogeneous computational chemistry data [version 1; peer review: 2 approved with reservations]. *F1000Research* **2020**, *9*.

(S16) Grimme, S. Supramolecular Binding Thermodynamics by Dispersion-Corrected Density Functional Theory. *Chemistry – A European Journal* **2012**, *18*, 9955–9964.

(S17) Li, Y.-P.; Gomes, J.; Mallikarjun Sharada, S.; Bell, A. T.; Head-Gordon, M. Improved Force-Field Parameters for QM/MM Simulations of the Energies of Adsorption for Molecules in Zeolites and a Free Rotor Correction to the Rigid Rotor Harmonic Oscillator Model for Adsorption Enthalpies. *The Journal of Physical Chemistry C* **2015**, *119*, 1840–1850.